

A Finite Element Analysis of Damaged Composite Sheet

Lect. Oday I. Abdullah

*Nuclear Engineering Dept., College of Eng.
Baghdad University, Baghdad, Iraq*

Lect. Ehsan Sabah M. Z. Ameen

*Mechanical Engineering Dept., College of Eng.
Al-Mustansiriya University, Baghdad, Iraq*

Eng. Wassan Safaa Abd Al-Sahb

*Mechanical Engineering Dept., College of Eng.
Al-Mustansiriya University, Baghdad, Iraq*

Abstract

This work is an attempt to study the behavior of a laminated composite sheet when subjected to specific damage cases and harmonic load. The numerical investigation is developed using finite element method with 8-nodes shell element to determine the free vibration and harmonic response by using the ANSYS package. The investigation covers three cases of damage laminate composite sheet with center impact loading.

The work procedure was to model a healthy structure and apply different damage cases in reference to the health structure in order to compute the shift in the stresses distribution in different layers. Damage occurs in several layers of the composite sheet in multiple locations throughout its volume, and through several layers of the sheet.

الخلاصة

هذا العمل محاولة لدراسة سلوك لوح مؤلف من صفائح رقيقة (الطبقات) متراكبة، عندما أخضع إلى حالات عيب معينة وتأثير قوى صدمة. تم التحقيق العددي باستخدام نظرية العناصر المحددة، واختيار العنصر القشري (8-عقد) للحصول على الترددات الطبيعية والاستجابة التوافقية باستخدام برنامج (ANSYS 5.4). البحث يغطي ثلاثة من حالات الضرر طبقت للوح المركب بتأثير حمل مركزي. خطوات العمل بدأت بعمل نموذج خالي من العيوب ثم طبقت حالات الضرر المختلفة لمعرفة التغيير في توزيع الإجهادات في الطبقات المختلفة. طبقت حالات الضرر المذكورة في عدة طبقات من اللوح المركب وفي مواقع مختلفة.

1. Introduction

The strength of structures materials can be reduced when subjected to high amplitude or repeated loads and, it may lead to failure over time with usage. This failure may be in several mechanisms. As various load conditions are applied to a composite element, the internal makeup can become damaged with mechanisms such as matrix cracking, delamination, fiber breakage, and local buckling. Primary matrix failure modes are characterized by cracks that run parallel to the fiber in plies that are not aligned with the principal tensile loading direction. Secondary matrix failure causes cracks that extend into adjacent plies, thus initiating delamination. A delamination, also called debonding, is a crack that extends within the resin rich (matrix material) interface between plies that may contain different fiber orientations. It has been observed that delamination only occurs in the presence of matrix cracks. As the delamination damage accumulates the material characteristics change until ultimately the structure fails in the form of fiber breakage^[1]. **Figure (1)** shows the characteristic progression of damage in a laminated composite. In the locations where failure begins to occur, the stiffness is reduced and the surrounding material must carry the load. Because the fibers are the load bearing material within a composite, when they fail the structure is permanently compromised.

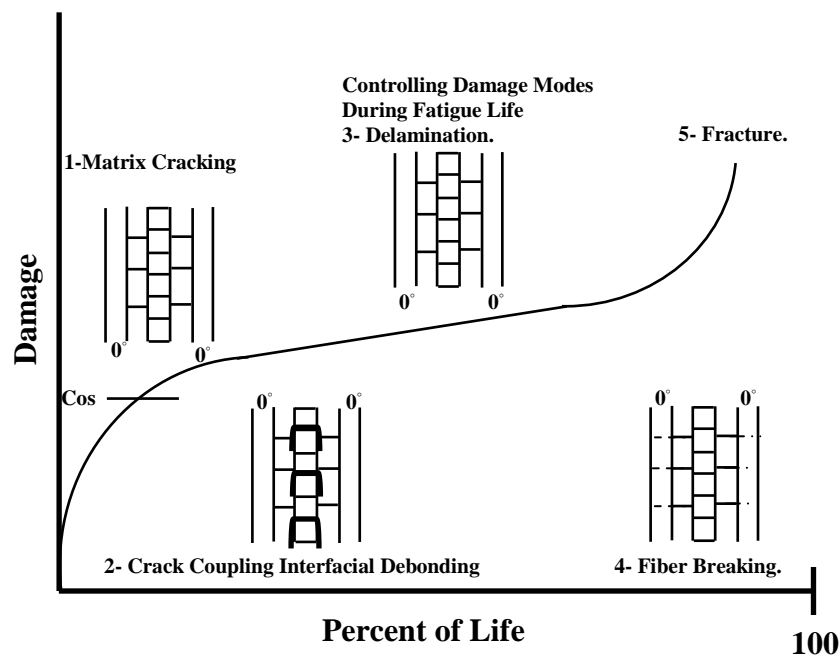


Figure (1) Development of damage in composite laminates

Failure takes place in stages, where one damage event can lead to a sequence of failures inside of the material as shown in the stress-strain curve in **Fig.(2)**. Failures within a ply are referred to as interlaminar and failures between layers are referred to as delamination. Each plateau in **Fig.(2)**, is a basic representation of a failure within a ply in a composite sheet. As consecutive ply failures occur, the end result is an overall failure of the composite laminate.

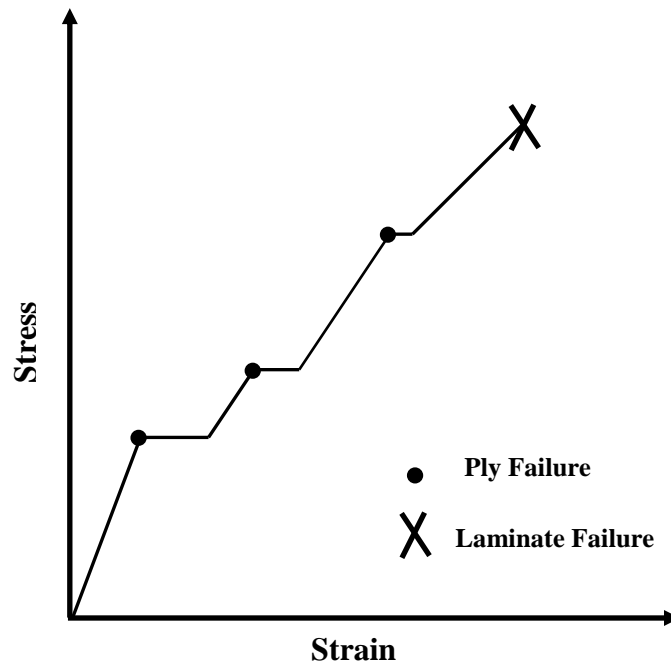


Figure (2) Failure process in laminate composite

The figure implies that the failure within a ply is sudden. But, in reality, the failure is progressive as mechanisms such as matrix cracking occur gradually rather than suddenly ^[2,3].

For the last three decades, understanding the effects of damage on composites has been the focus of many studies. A few of those studies are mentioned here.

Engblom and Havelka ^[4] used a combined analytical and experimental approach to develop models of damaged composite structures. The experimentation was intended to quantify the effects of the four major damage mechanisms on the variations in stiffness and damping characteristics. The data gained from the experiments were used to improve existing finite element based damage models, as well as improve predictions of changes in material properties. The result of their work indicated that the effects of delamination and matrix cracking can greatly affect the residual properties and dynamic characteristics of laminated composites. In order to differentiate between the various failure mechanisms, failure criteria, developed by other researchers, were incorporated in the assessment of the damage.

Hashin ^[5] developed a stress based failure criteria to distinguish between fiber and matrix failure modes. Lee ^[6] used a similar stress based criteria to distinguish delamination from other failure modes.

Yen, Cassin, Patterson, and Triplett ^[7] conducted a progressive failure analysis of thin walled composite tubes under low energy impact. This study was also a comparative study of experimental and analytical analyses. The failure criteria developed therein was integrated into an explicit dynamic analysis code for failure prediction of the composite tubes. The results provided a good correlation with experimental data of impact force histories and certain critical damage modes. Also, the code predicted nonlinear behavior due to the progression of local damage, within the macroscopic continuum.

Talreja ^[1] developed an internal state variable model, which was used to determine the overall stiffness properties and intensity of damage in individual modes. This relationship shows that interlaminar damage reduces all the elastic moduli for damage with general orientations and changes the initial orthotropic symmetry of a laminate. But the interlaminar damage does not change the symmetry, only the moduli. This model represents the effects of matrix cracking on stiffness reduction by evaluating the development of crack size within the ply. Then, the model characterizes the damage modes as factorial quantities that incorporate the geometrical properties of the damage entities.

Jonathan ^[3] presented the effects of various damage cases, load input locations, and frequency spectra on the dynamic response of a laminated composite sheet. A realistic finite element model generated using material properties and dynamic characteristics. Jonathan used the results of the model to provide insight into the progression and accumulation of damage within the plies of the composite sheet.

In this work, jonathan's work is continued with different damage cases and different loads and locations.

2. Mathematical Representation of Laminated Composites and Loading

The response and characteristics of laminated composites are governed by many equations. A laminated sheet with a thickness that is small compared to the lateral dimensions has displacement components u , v , and w that are functions of x , y , and z .

These equations are expanded in terms of the power series of z . Because the displacements are small, only the first two terms in the series are retained. The first terms are identified as the displacement components of the mid-plane, the second terms represent the linear relationship with the deformation in the z direction:

$$\begin{aligned}
 \mathbf{u}(\mathbf{x}, \mathbf{y}, \mathbf{z}) &= \mathbf{u}_0(\mathbf{x}, \mathbf{y}) + \mathbf{z}\phi_x(\mathbf{x}, \mathbf{y}) \\
 \mathbf{v}(\mathbf{x}, \mathbf{y}, \mathbf{z}) &= \mathbf{v}_0(\mathbf{x}, \mathbf{y}) + \mathbf{z}\phi_x(\mathbf{x}, \mathbf{y}) \dots\dots\dots (1) \\
 \mathbf{w}(\mathbf{x}, \mathbf{y}, \mathbf{z}) &= \mathbf{w}_0(\mathbf{x}, \mathbf{y})
 \end{aligned}$$

In general, the stress-strain relation, $\{\mathbf{s}\}$ and $\{\mathbf{e}\}$, of a lamina (ply) is governed by the elastic compliance matrix $[\mathbf{S}]$, which is the inverse of the elastic constant matrix $[\mathbf{C}]$:

$$\{\mathbf{\epsilon}\} = [\mathbf{C}]^{-1} \{\mathbf{\sigma}\} = [\mathbf{S}]\{\mathbf{\sigma}\} \dots\dots\dots (2)$$

Where the matrix $[\mathbf{S}]$ is determined by the mechanical properties of the lamina ^[2]:

$$[S] = \begin{bmatrix} \frac{1}{E_x} & -\frac{\nu_{yx}}{E_y} & -\frac{\nu_{zx}}{E_z} & \frac{\eta_{yx,x}}{G_{yz}} & \frac{\eta_{xz,x}}{G_{xz}} & \frac{\eta_{xy,x}}{G_{xy}} \\ \frac{\nu_{xy}}{E_x} & \frac{1}{E_y} & -\frac{\nu_{zy}}{E_z} & \frac{\eta_{yz,y}}{G_{yz}} & \frac{\eta_{xz,x}}{G_{xz}} & \frac{\eta_{xy,x}}{G_{xy}} \\ -\frac{\nu_{xz}}{E_z} & -\frac{\nu_{yz}}{E_y} & \frac{1}{E_z} & \frac{\eta_{yz,z}}{G_{yz}} & \frac{\eta_{xz,z}}{G_{xz}} & \frac{\eta_{xy,x}}{G_{xy}} \\ \frac{\eta_{x,yz}}{E_x} & \frac{\eta_{y,yz}}{E_y} & \frac{\eta_{z,yz}}{E_z} & \frac{1}{G_{yz}} & \frac{\mu_{xz,yz}}{G_{xz}} & \frac{\mu_{xy,yz}}{G_{xy}} \\ \frac{\eta_{x,xz}}{E_x} & \frac{\eta_{y,xz}}{E_y} & \frac{\eta_{z,xz}}{E_z} & \frac{\mu_{yz,xz}}{G_{yz}} & \frac{1}{G_{xz}} & \frac{\mu_{xy,xz}}{G_{xy}} \\ \frac{\eta_{z,xy}}{E_x} & \frac{\eta_{y,xy}}{E_y} & \frac{\eta_{z,xy}}{E_z} & \frac{\mu_{yz,xy}}{G_{yz}} & \frac{\mu_{xz,xy}}{G_{xz}} & \frac{1}{G_{xy}} \end{bmatrix} \dots\dots\dots (3)$$

The stress-strain relation for orthotropic materials is simplified due to the symmetric property of the compliance matrix and follows the relationship:

$$\begin{Bmatrix} \epsilon_{11} \\ \epsilon_{22} \\ \epsilon_{33} \\ \gamma_{23} \\ \gamma_{13} \\ \gamma_{12} \end{Bmatrix} = \begin{bmatrix} \frac{1}{E_1} & -\frac{\nu_{21}}{E_2} & -\frac{\nu_{31}}{E_3} & 0 & 0 & 0 \\ \frac{\nu_{12}}{E_1} & \frac{1}{E_2} & -\frac{\nu_{32}}{E_3} & 0 & 0 & 0 \\ -\frac{\nu_{13}}{E_1} & -\frac{\nu_{23}}{E_2} & \frac{1}{E_3} & 0 & 0 & 0 \\ 0 & 0 & 0 & \frac{1}{G_{23}} & 0 & 0 \\ 0 & 0 & 0 & 0 & \frac{1}{G_{13}} & 0 \\ 0 & 0 & 0 & 0 & 0 & \frac{1}{G_{12}} \end{bmatrix} \begin{Bmatrix} \sigma_{11} \\ \sigma_{22} \\ \sigma_{33} \\ \sigma_{23} \\ \sigma_{13} \\ \sigma_{12} \end{Bmatrix} \dots\dots\dots (4)$$

Although the strains are continuous over the thickness of the laminate, the stresses in the laminate are discontinuous across the interfaces due to the different material properties resulting from different fiber orientations. For the kth lamina, the stress components are given by Sun [2].

$$\begin{Bmatrix} \sigma_{xx} \\ \sigma_{yy} \\ \sigma_{xy} \end{Bmatrix} = \begin{bmatrix} \overline{Q}_{11} & \overline{Q}_{12} & \overline{Q}_{16} \\ \overline{Q}_{12} & \overline{Q}_{22} & \overline{Q}_{26} \\ \overline{Q}_{16} & \overline{Q}_{26} & \overline{Q}_{66} \end{bmatrix}_k \left[\begin{Bmatrix} \epsilon_x^\circ \\ \epsilon_y^\circ \\ \epsilon_z^\circ \end{Bmatrix} + z \begin{Bmatrix} k_x \\ k_y \\ k_{xy} \end{Bmatrix} \right] \dots\dots\dots (5)$$

Eq.(5), [Q] represents the reduced stiffness, a term similar to the elastic constants, which is the inverse of the elastic compliance. The strains are described by the in-plane strain and curvatures due to bending in the sheet. Typically, the strains associated with bending have the

most significant effect. In composites this is influenced by the stacking sequence of the laminate.

When evaluating the strength within a lamina, there are several criteria that can be used. One such criterion is the Maximum Stress Criterion, which compares the maximum tensile strength in the fiber direction, transverse to the fiber direction, in-plane shear strength to the state of stress found in the structure.

Eq.(6) presents the motion:

$$[M]\{\ddot{U}\}+[C]\{\dot{U}\}+[K]\{U\} = \{R\} \dots\dots\dots (6)$$

This can be solved by a harmonic analysis; therefore, the displacement may be defined as:

$$\{U\} = \{U_o (\cos(\Phi) + U_o i \sin(\Phi))\} e^{i\Omega t} \dots\dots\dots (7)$$

Also, the force vector can be specified analogously to the displacement vector:

$$\{R\} = \{R_o (\cos(\Psi) + i \sin(\Psi))\} e^{i\Omega t} \dots\dots\dots (8)$$

where,

$U_o =$ Maximum displacement (mm).

$i =$ Square root of (-1).

$\Omega =$ Imposed circular frequency (rad / sec).

$\Phi =$ Displacement phase shift (rad).

$t =$ Time (sec)

$R_o =$ Force amplitude (N).

$\Psi =$ Force phase shift (rad).

$\{R_1\} = \{R_o \cos(\Psi)\} =$ Real force vector.

$\{R_2\} = \{R_o \sin(\Psi)\} =$ Imaginary force vector.

$\{U_1\} = \{U_o \cos(\Phi)\} =$ Real displacement vector.

$\{U_2\} = \{U_o \sin(\Phi)\} =$ Imaginary displacement vector.

When $\{R_2\} = 0$ and re-arranging eq.(6), substituting eqs.(7) and (8) we get eq.(9):

$$([K] - \Omega^2 [M] + i \Omega [C]) (\{U_1\} + i \{U_2\}) = \{R_o\} \dots\dots\dots (9)$$

Solving eq.(9) gives the displacement component U_1 and U_2 .

3. Description of the Case Study

The model was based on a 20-ply composite sheet with S2 Glass/Epoxy for the fiber and matrix material in each of the plies. The laminated sheet is symmetric about the mid-plane with a stacking sequence of $[(0/90)_{10}]_s$. The overall dimensions used for this model are 1.219m x 0.914m x 6.35mm. The thickness of each ply is uniform at 0.3175mm.

The material properties ^[2] used in modeling the sheet:

$$E_x = 43.3 \text{ GPa}, E_y = 12.7 \text{ GPa}, E_z = 12.7 \text{ GPa}, \nu_{xy} = 0.29, \nu_{yz} = 0.5, \nu_{xz} = 0.29,$$

$$G_{xy} = 4.5 \text{ GPa}, G_{yz} = 2 \text{ GPa}, G_{xz} = 4.5 \text{ GPa}, \rho = 1800 \text{ Kg/m}^3$$

The three dimensional [shell99] (520) elements are used in this analysis. The stresses and deformations are computed for different mesh models, it is preferable to name the suitable mesh size to be used during the analysis. In each of the simulations, all of the edges of the sheet were constrained in all six degrees of freedom.

The force on the sheet was applied as a distributed load over an area of 0.0247m² with a magnitude 2500 N (The total force on the sheet). This value is a reasonable estimate of loading from a ballistic impact ^[3]. The boundary conditions are shown in **Fig.(3)**.

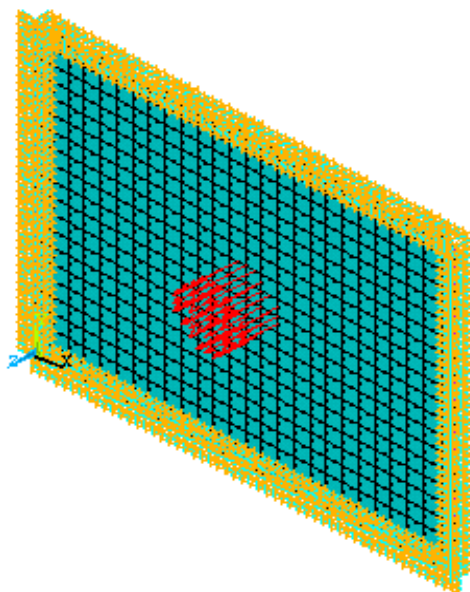


Figure (3) The health case study (constraint and load conditions)

4. Verification Test

The current results are compared with the results of ^[3] numerical study as exhibited in **Table (1)**, which demonstrates the first five natural frequencies of the same case study. The maximum difference is less than 0.07%.

Table (1) Values of the first five natural frequencies (Hz) for the composite sheet (Health case study)

Mode No.	Present Work	Ref. (Jonathan, 2003)	%Difference
1	36.99	36.97	0.054
2	62.85	62.82	0.047
3	87.28	87.22	0.068
4	106.23	106.16	0.065
5	108.16	108.13	0.027

5. Simulation of Damage

The method used to simulate damage in the composite model was to assume that the modulus and shear modulus were nearly zero at the location of damage. In order to avoid singularity issues during calculation, the properties were not set exactly to zero. For all damage cases, the material properties assigned to those locations were as follows:

$$E_x = E_y = E_z = 80 \text{ Pa}, G_{xy} = G_{yz} = G_{xz} = 40 \text{ Pa}, \nu_{xy} = \nu_{yz} = \nu_{xz} = 0.3$$

These properties are significantly less than those of a healthy structure. The strength in damaged regions is decreased by a factor of 10^8 , which essentially acts as zero. These properties represent the effect of a total failure of the load carrying capability of that region. The initial effects of damage are difficult to model. For example no stiffness reduction is assumed after primary matrix failure occurs. This is because, transverse matrix cracks alone usually do not have a significant effect on the laminate stiffness.

The damage and force locations are shown in **Fig. (4)**. In this figure, the square shapes represent the regions in which damage occurs, and the circles represent the distributed force. The details of each damage case are outlined in **Table (2)**.

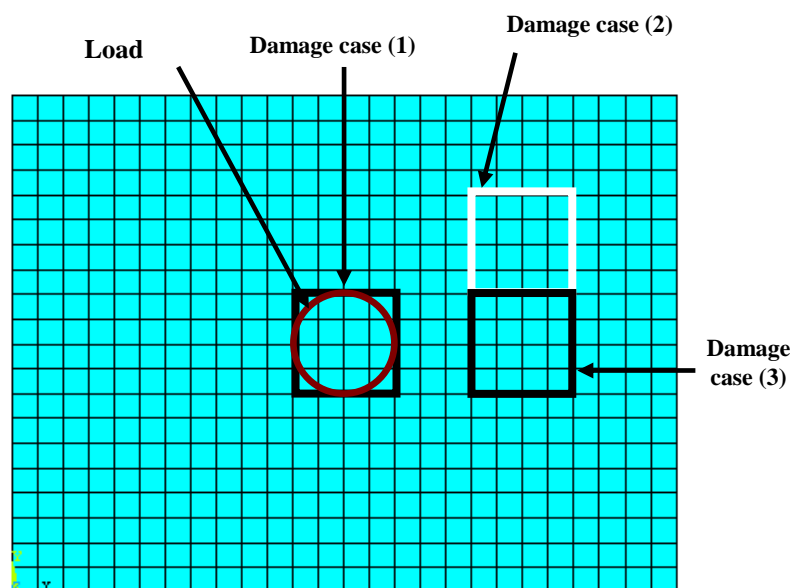


Figure (4) Damage and force locations on composite sheet, all sides are fixed

6. Results and Discussions

The first step in evaluating the response of the laminated composite sheet was to perform a modal analysis. The plate was set with the same boundary conditions which used for the harmonic forced response. All four edges of the sheet were fully constraint in all degrees of freedom. The first five natural frequencies for the healthy and damaged cases are shown in **Table. (3)**. It can be noticed from the table that, when the damage is applied, the change in the values of natural frequencies is very small. The maximum percentage difference is not to exceed 1.27 % in fundamental natural frequency.

The second set of results is the harmonic analysis. All results were found within a frequency range of 30 to 120 Hz. This range was determined by the first and last natural mode of the sheet, the force is applied as a step load with a zero phase angle. Also a constant damping ratio of (0.1) ^[2] is applied to the entire model.

For the healthy case, **Figs.(5, 9, 13, 17, 21 and 25)** show the Von-Mises stresses versus frequency corresponding to the layers (1, 2, 3, 14, 15 and 16) respectively. The peak stress occurs in the range of 37 Hz at the 2nd layer, with a magnitude of about 56 MPa.

For case (1), **Figs.(6, 10, 14, 18, 22, and 26)** demonstrate the variation of the Von-Mises stresses with the variation of frequency corresponding to the layers (1, 2 and 3) above the damage region and (14, 15 and 16) below the damaged region respectively. The peak stress is in the range of 36 Hz in the 2nd layer, with a magnitude of about 305 MPa.

Figures (7, 11, 15, 19, 23, and 27) show the Von-Mises stresses versus frequency for damage case (2), corresponding to the layers (1, 2 and 3) above the damage region and (14, 15 and 16) below the damaged region respectively. The maximum stress is in the range of 37 Hz in the 2nd layer, with a peak magnitude of about 72 MPa.

Finally, for damaged case (3), **Fig. (8, 12, 16, 20, 24, and 28)** show the variation of the Von-Mises stresses with the variation of frequency corresponding to the layers (1, 2 and 3) above the damage region and (14, 15 and 16) below the damaged region respectively. The maximum stress is in the range of 38 Hz in the 2nd layer, with a peak magnitude of about 141 MPa.

From above it can be found that, the overall trend of the stress (as it is distributed through the layers) decreases from the outer surfaces to the mid-plane. But, due to the damage, the stress in the first three layers increases because of the reduction in the local cross-sectional area. Also, the peak stresses in bottom three layers do not exceed that of the top three layers.

Besides to the change in magnitude of stress in the sheet, there is also a slight shift in the frequency at which the peak stresses occur. For the first mode, the frequency shifted down 1 Hz for case (1), no frequency shifted down for case (2) and up 1 Hz for case (3).

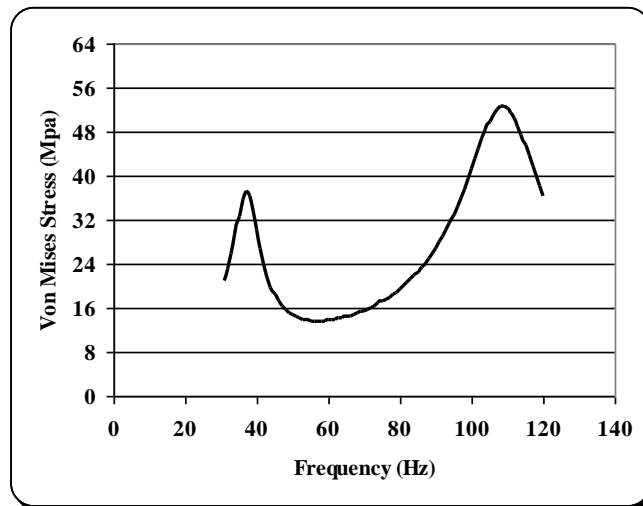


Figure (5) The Values of Von-Mises stresses with the frequency for the 1st layer (Health case)

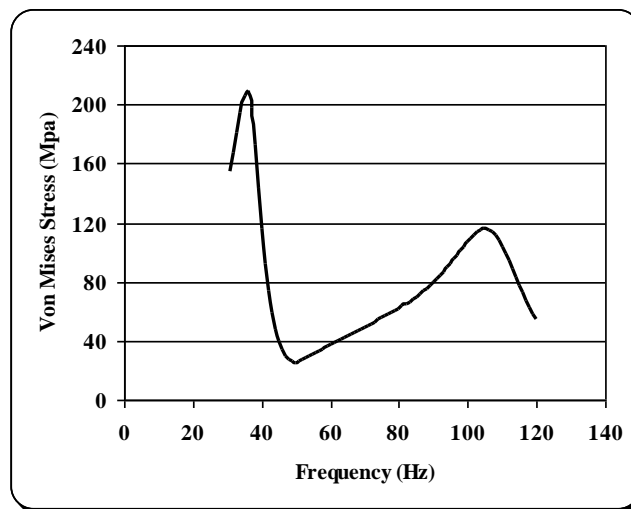


Figure (6) The Values of Von-Mises stresses with the frequency for the 1st layer (case one)

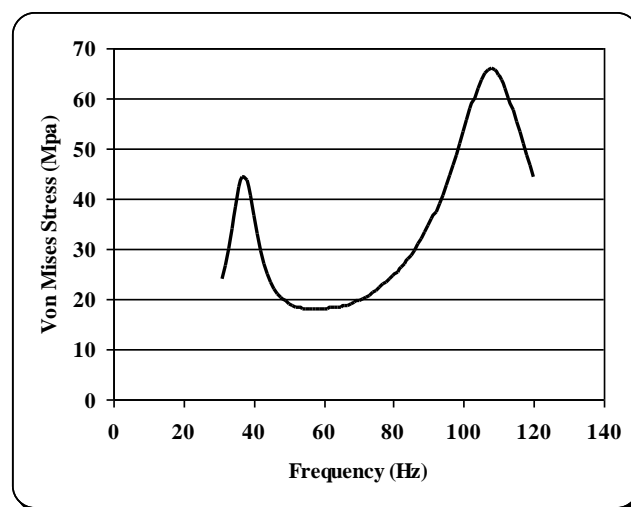


Figure (7) The Values of Von-Mises stresses with the frequency for the 1st layer (case Two)

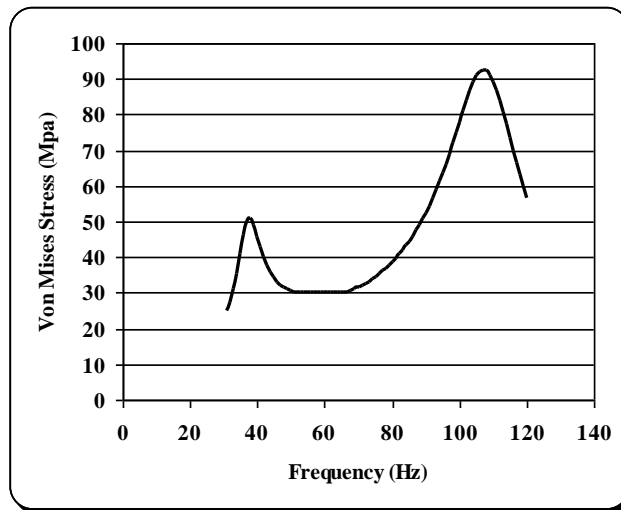


Figure (8) The Values of Von-Mises stresses with the frequency for the 1st layer (case three)

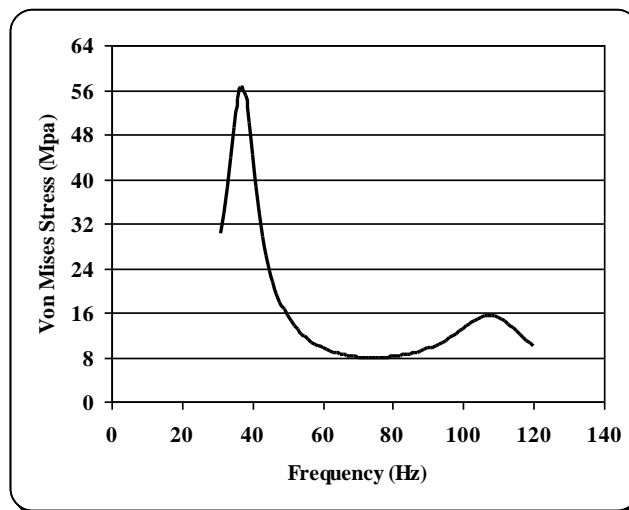


Figure (9) The Values of Von-Mises stresses with the frequency for the 2nd layer (Health case)

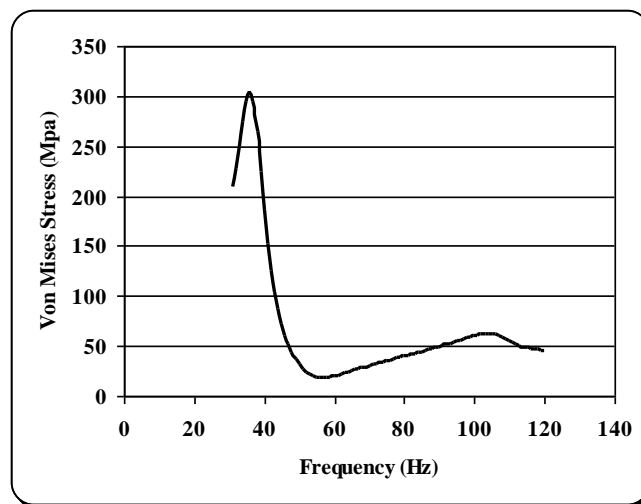


Figure (10) The Values of Von-Mises stresses with the frequency for the 2nd layer (case one)

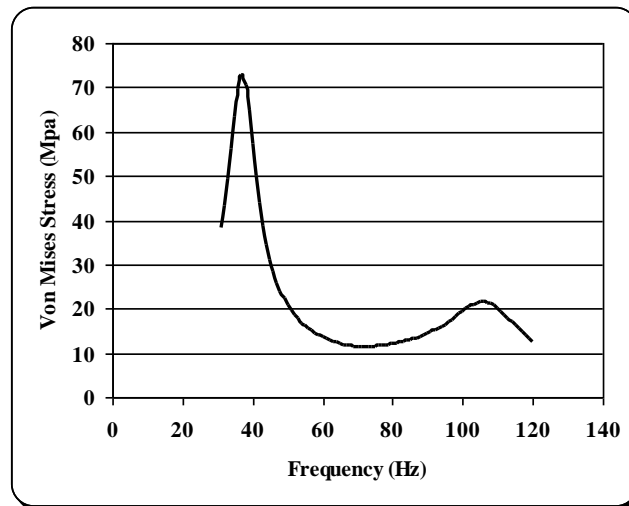


Figure (11) The Values of Von-Mises stresses with the frequency for the 2nd layer (case two)

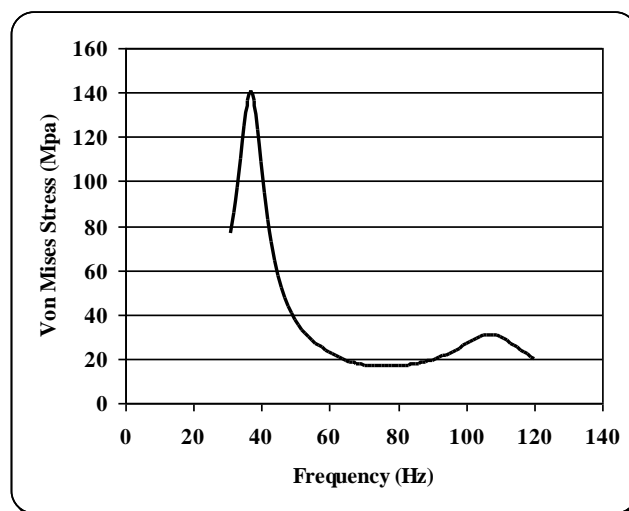


Figure (12) The Values of Von-Mises stresses with the frequency for the 2nd layer (case three)

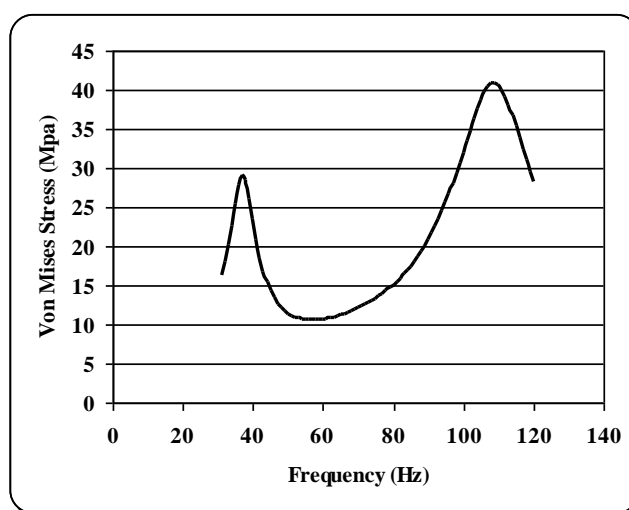


Figure (13) The Values of Von-Mises stresses with the frequency for the 3rd layer (Health case)

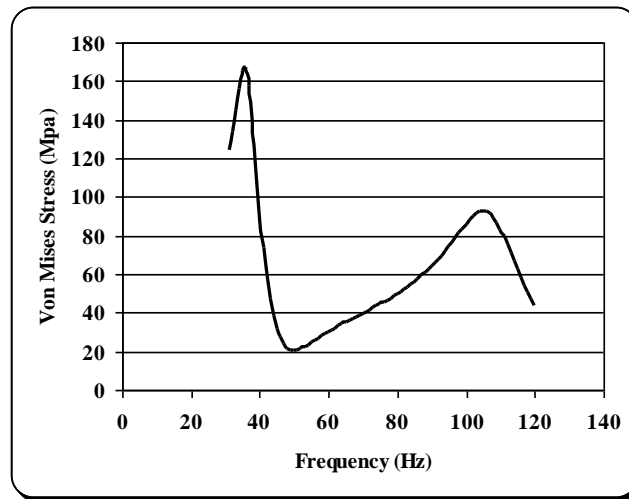


Figure (14) The Values of Von-Mises stresses with the frequency for the 3rd layer (case one)

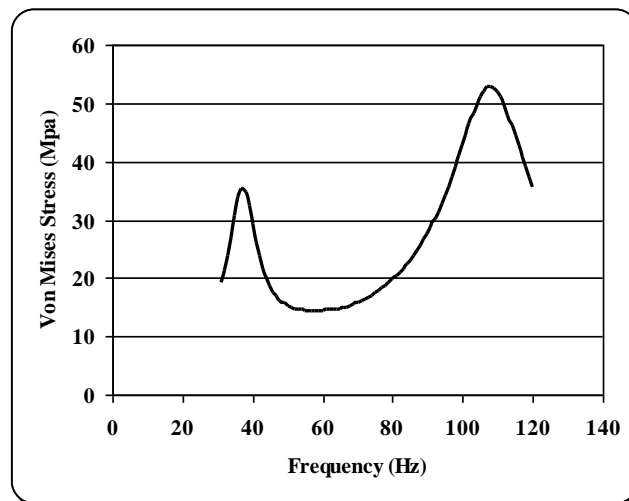


Figure (15) The Values of Von-Mises stresses with the frequency for the 3rd layer (case two)

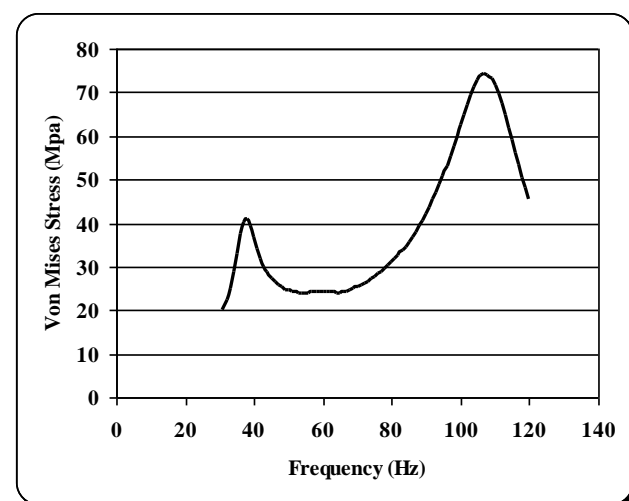


Figure (16) The Values of Von-Mises stresses with the frequency for the 3rd layer (case three)

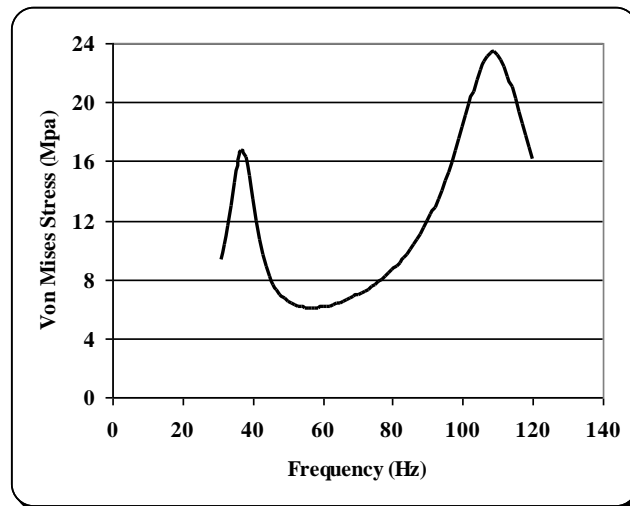


Figure (17) The Values of Von-Mises stresses with the frequency for the 14th layer (Health case)

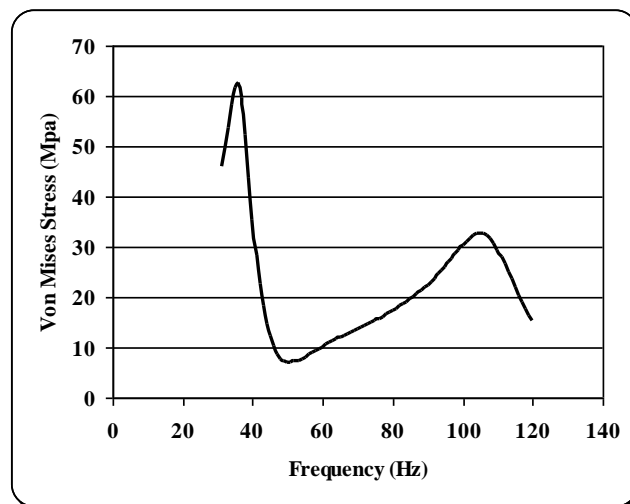


Figure (18) The Values of Von-Mises stresses with the frequency for the 14th layer (case one)

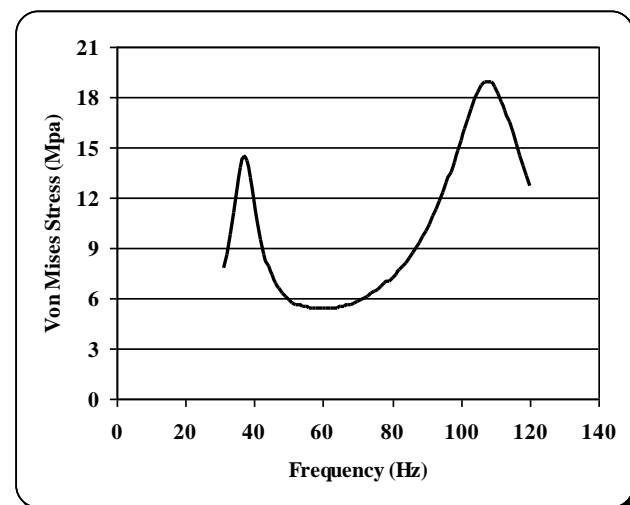


Figure (19) The Values of Von-Mises stresses with the frequency for the 14th layer (case two)

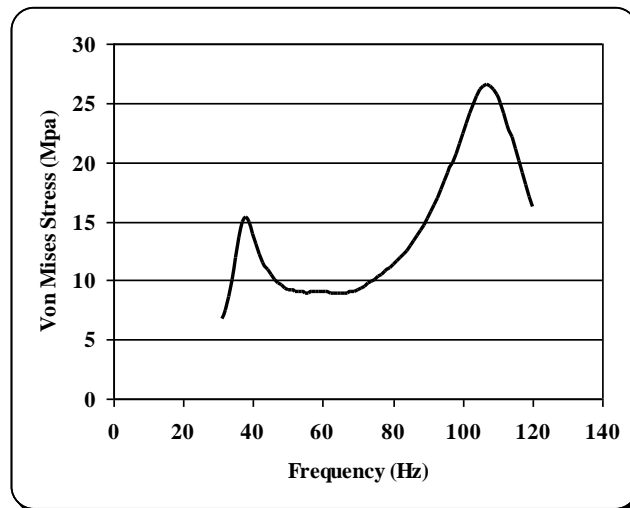


Figure (20) The Values of Von-Mises stresses with the frequency for the 14th layer (case three)

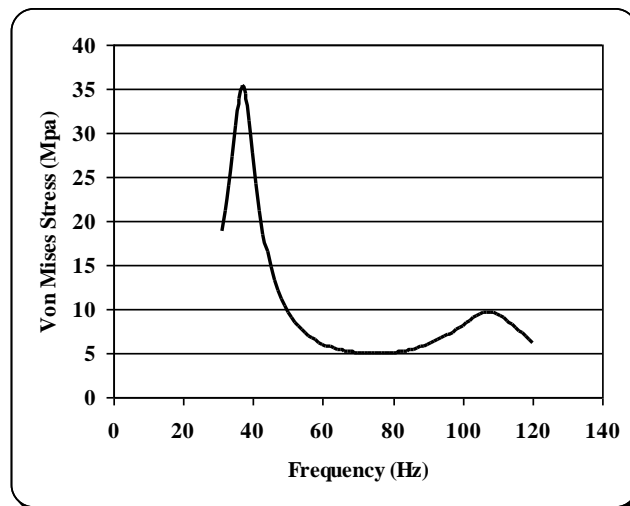


Figure (21) The Values of Von-Mises stresses with the frequency for the 15th layer (Health case)

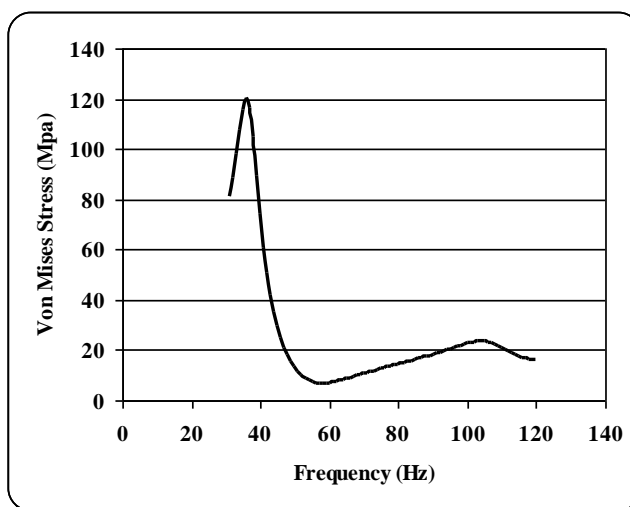


Figure (22) The Values of Von-Mises stresses with the frequency for the 15th layer (case one)

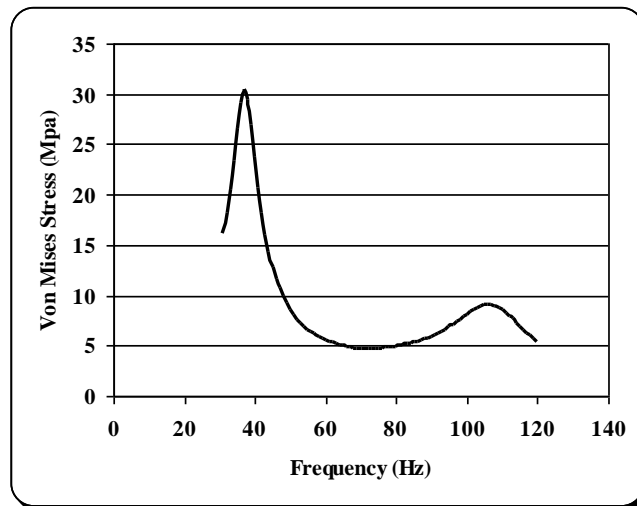


Figure (23) The Values of Von-Mises stresses with the frequency for the 15th layer (case two)

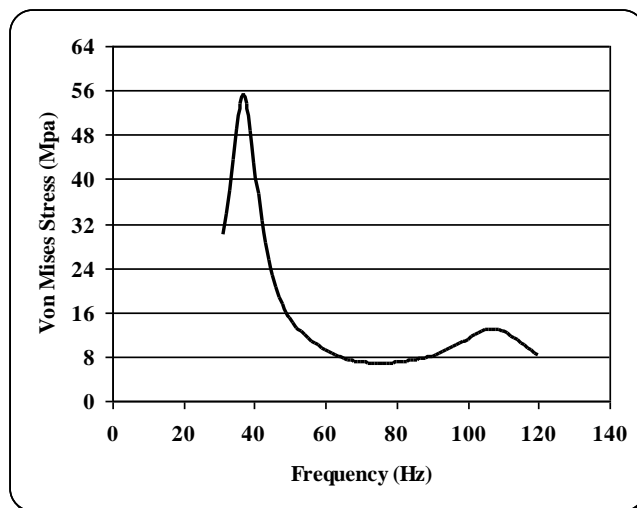


Figure (24) The Values of Von-Mises stresses with the frequency for the 15th layer (case three)

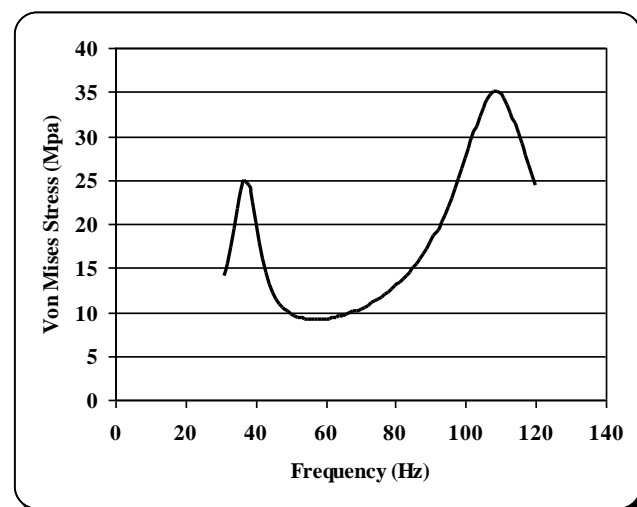


Figure (25) The Values of Von-Mises stresses with the frequency for the 16th layer (Health case)

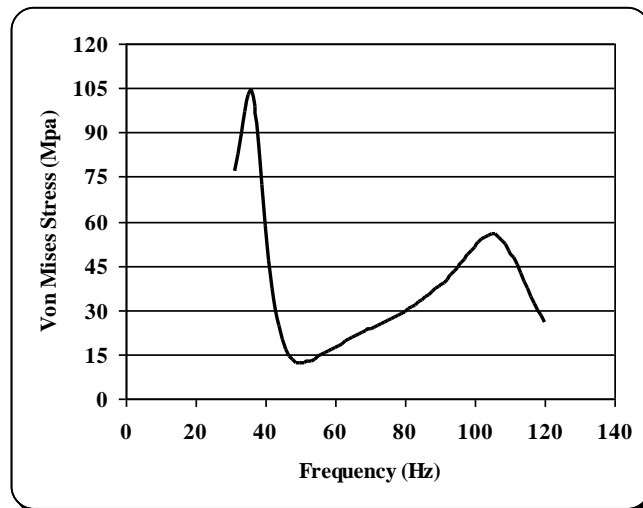


Figure (26) The Values of Von-Mises stresses with the frequency for the 16th layer (case one)

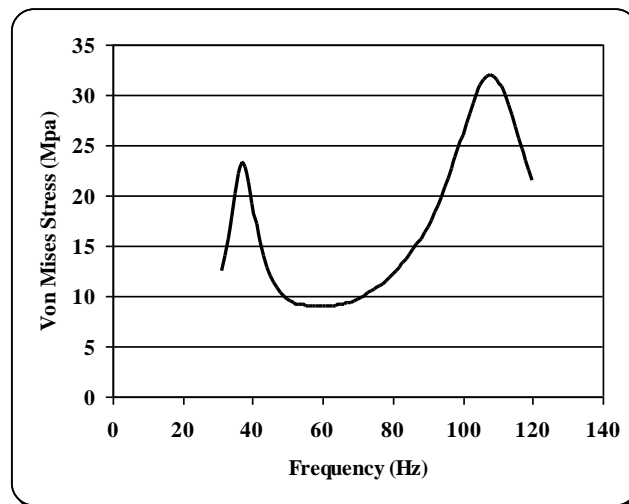


Figure (27) The Values of Von-Mises stresses with the frequency for the 16th layer (case two)

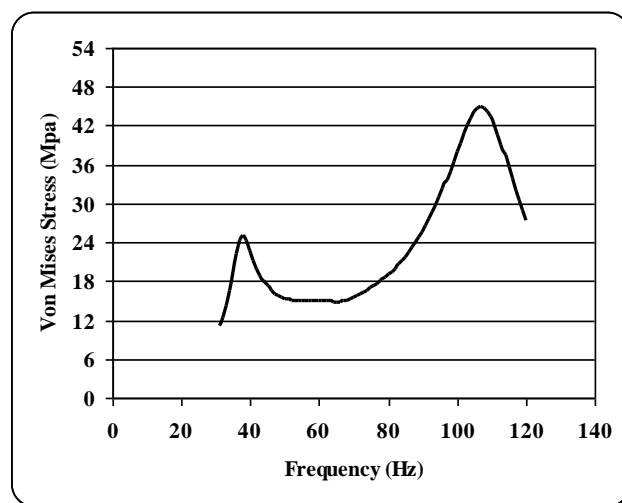


Figure (28) The Values of Von-Mises stresses with the frequency for the 16th layer (case three)

7. Conclusions

The above analysis leads to the following conclusions: (The first two agree with those concluded by Jonathan ^[3]).

1. For all cases the stress in the top layers, just above the damage, is higher than those just below. This is attributed to the reduction in the local cross-sectional area.
2. In some cases the stress around the damaged area increases or decreases. The areas of increase indicate the load-carrying path of the structure in that region.
3. When the load applied at the center of the damage, this location faces the largest stress (case-1). (This result is expected but, the large change in the stress range is not expected).

8. References

1. Talreja, R., "*Stiffness Properties of Composite Laminates with Matrix Cracking and Interior Delamination*", Engineering Fracture Mechanics, Vol. 25, No. 5/6, 1986, pp. 751-762.
2. Sun, C. T., "*Mechanics of Composite Materials and Laminates*", Lecture Notes A&AE 555, Spring 2003, Purdue University.
3. Jonathan, F. Wenk, "*A Finite Element Analysis of Damage Accumulation in Heterogenous Structures*", M.Sc. Thesis, Purdue University, 2003.
4. Engblom, J. J., Havelka, J. J., "*Combined Analytical/Experimental Approach for Developing Structural Model of Damaged Composite Structures*", AIAA Conference, American Institute of Aeronautics and Astronautics, AIAA-91-1085-CP, 1991.
5. Hashin, Z., "*Failure Criteria for Unidirectional Fiber Composites*", Journal of Applied Mechanics, V. 47, 1980, pp. 329-334.
6. Lee, J. D., "*Three Dimensional Finite Element Analysis of Damage Accumulation in Composite Laminates*", Computers and Structures, Vol. 15, No. 3, 1982, pp. 335-350.
7. Yen, C., Cassin, T., Patterson, J., Triplett, M., "*Progressive Failure of Thin Walled Composite Tubes under Low Energy Impact*", U.S Army Missile Command, 1997.

List of Symbols

Symbol	Definition	Units
[S]:	Elastic compliance matrix.	
[C]:	The inverse of the elastic constant matrix.	
$\varepsilon_{11}, \varepsilon_{22}, \varepsilon_{33}$:	Normal strains.	
δt :	Time interval.	Second
F:	Impact force.	N
σ_{xx} :	The stress in the X-Direction.	N/m ²
σ_{yy} :	The stress in the Y-Direction.	N/m ²
σ_{xy} :	The stress in the X-Direction on the Y facing face.	N/m ²
E_x :	Young's modules in X-direction.	N/m ²
E_y :	Young's modules in Y-direction.	N/m ²
E_z :	Young's modules in Z-direction.	N/m ²
ν_{xy} :	Poisson's ratio, the strain in the x-direction due to strain in the y-direction.	
ν_{yx} :	Poisson's ratio, the strain in the y-direction due to strain in the x-direction.	
ν_{zx} :	Poisson's ratio, the strain in the z-direction due to strain in the x-direction.	
ν_{zy} :	Poisson's ratio, the strain in the z-direction due to strain in the y-direction.	
ν_{xz} :	Poisson's ratio, the strain in the x-direction due to strain in the z-direction.	
ν_{yz} :	Poisson's ratio, the strain in the y-direction due to strain in the z-direction.	
G_{xy}, G_{xz}, G_{yz} :	Shearing modules	N/m ²
$\gamma_{23}, \gamma_{13}, \gamma_{12}$:	Searing strains	
σ_m :	Mean stress	N/m ²
σ_a :	Alternating stress	N/m ²
N_f :	Safety factor	
S_{ut} :	Ultimate stress	N/m ²